

1 **Redundant and Distinct Roles of Secreted Protein Eap and Cell Wall-Anchored**
2 **Protein SasG in Biofilm Formation and Pathogenicity of *Staphylococcus aureus***

3

4 Running Title: Roles of Eap and SasG in Biofilm and Pathogenesis

5

6 Keigo Yonemoto,^{a,b,c} Akio Chiba,^{a,b} Shinya Sugimoto,^{a,b,#} Chikara Sato,^d Mitsuru Saito,^c

7 Yuki Kinjo,^{a,b} Keishi Marumo,^{b,c} and Yoshimitsu Mizunoe^{a,b}

8 ^aDepartment of Bacteriology, The Jikei University School of Medicine, Tokyo, Japan

9 ^bJikei Center for Biofilm Science and Technology, The Jikei University School of Medicine,
10 Tokyo, Japan

11 ^cDepartment of Orthopaedic Surgery, The Jikei University School of Medicine, Tokyo,
12 Japan

13 ^dBiomedical Research Institute, National Institute of Advanced Industrial Science and
14 Technology (AIST), Ibaraki, Japan

15

16 #Address correspondence to Shinya Sugimoto, ssugimoto@jikei.ac.jp.

17 K.Y. and A.C. contributed equally to this work.

18 **ABSTRACT**

19 Chronic and fatal infections caused by *Staphylococcus aureus* are sometimes associated
20 with biofilm formation. Secreted proteins and cell wall-anchored proteins (CWAPs) are
21 important for the development of polysaccharide-independent biofilms, but functional
22 relationships between these proteins are unclear. In the current study, we report the roles
23 of the extracellular adherence protein Eap and surface CWAP SasG in *S. aureus* MR23,
24 a clinical methicillin-resistant isolate that forms a robust protein-dependent biofilm and
25 accumulates a large amount of Eap in the extracellular matrix. Double-deletion of *eap*
26 and *sasG*, but not single *eap* or *sasG* deletion, reduced biomass of the formed biofilm.
27 Mutational analysis demonstrated that cell wall-anchorage is essential for the role of
28 SasG in biofilm formation. Confocal laser scanning microscopy revealed that MR23
29 formed a rugged and thick biofilm; deletion of both, *eap* and *sasG*, reduced biofilm
30 ruggedness and thickness. Although *sasG* deletion did not affect either of these features,
31 *eap* deletion reduced the ruggedness but not thickness of the biofilm. This indicated that
32 Eap contributes to the rough irregular surface structure of the MR23 biofilm, and that both
33 Eap and SasG play a role in biofilm thickness. The pathogenicity of $\Delta eap \Delta sasG$ strain in
34 a silkworm larval infection model was significantly lower ($P < 0.05$) than that of the
35 wild-type and single-deletion mutants. Collectively, these findings highlight the redundant

36 and distinct roles of a secreted protein and a CWAP in biofilm formation and
37 pathogenicity of *S. aureus* and may inform new strategies to control staphylococcal
38 biofilm infections.

39 **INTRODUCTION**

40 Biofilms are recognized as the dominant form of life of microbes on Earth (1, 2).
41 Pathogenic and commensal bacteria that form biofilms in the human body or artificial
42 implants can cause chronic infections (3, 4). Since bacteria embedded within biofilms
43 acquire tolerance to host immunity and antibacterial drugs (5), biofilm-associated
44 infections are difficult to treat, can be life-threatening, and increase treatment costs in the
45 clinical setting (6). To combat biofilm-associated issues, understanding the molecular
46 mechanisms of biofilm formation and development of strategies to control biofilm
47 formation based on the gained mechanistic insights are pivotal.

48 *Staphylococcus aureus* is a commensal bacterium carried by approximately 30%
49 of healthy population (7, 8). It is an opportunistic pathogen that causes various infectious
50 diseases, from superficial skin infections to invasive infections (9, 10). *S. aureus* can also
51 cause chronic infections associated with biofilms (11). Within biofilms, bacterial cells are
52 embedded in an extracellular matrix (ECM) comprised of DNA, polysaccharides, and/or
53 proteins (12), but the amount of each component differs depending on the strain and
54 culture conditions (13). Extracellular DNA (eDNA) is important for the primary attachment
55 of cells to the substratum, and contributes to the maintenance of biofilm structure in both
56 gram-negative bacteria and gram-positive bacteria, including *S. aureus* (14–16). Specific

57 polysaccharides, i.e., polysaccharide intercellular adhesin (PIA) or
58 poly-*N*-acetylglucosamine, play an important role in *S. aureus* biofilms (17–19). On the
59 other hand, certain strains produce PIA-independent and protein-dependent biofilms (20),
60 mainly relying on either secreted proteins or cell wall-anchored proteins (CWAPs) (12).

61 Extracellular adherence protein (Eap), also known as MHC class II analog
62 protein (Map), is an *S. aureus*-specific secreted protein (21). Eap contributes to the
63 virulence of *S. aureus* by facilitating interactions between the bacterial cell surface and
64 several plasma proteins, thus promoting adherence to the host endothelium and
65 internalization into human fibroblasts and epithelial cells (22, 23). Eap plays an important
66 role in biofilm formation under certain growth conditions (24, 25). Disruption of the *eap*
67 gene in *S. aureus* Newman leads to a slight reduction of biofilm formation under low-iron
68 conditions (24). Further, deletion of *eap* remarkably reduces biofilm formation by *S.*
69 *aureus* SA113 (ATCC 35556) derived from the laboratory strain NCTC8325, under
70 iron-replete conditions in the presence of human serum (25).

71 CWAPs are classified into four distinct groups (26). The first group belongs to the
72 microbial surface component-recognizing adhesive matrix molecules and includes
73 clumping factors (ClfA and ClfB) and fibronectin binding proteins (FnBPA and FnBPB).
74 Proteins from the second group harbor the near-iron transporter motif and include

75 iron-regulated surface determinant proteins (IsdA, IsdB, and IsdH). The third group
76 proteins contain tandemly repeated three helical bundles, e.g., protein A. The fourth
77 group comprises the G5-E repeat family proteins, including *S. aureus* surface protein G
78 (SasG). All CWAPs contain a characteristic five-amino acid structure called the LPXTG
79 motif (Leu-Pro-any amino acid-Thr-Gly) (27). The LPXTG motif is recognized by the
80 membrane protein sortase A (SrtA) (27), which cleaves the peptide bond between
81 threonine and glycine residues and covalently bridges the threonine to lipid II, a precursor
82 of peptidoglycan (28). Although extensive efforts have been made to demonstrate the
83 individual importance of these proteins in biofilm formation and pathogenesis, functional
84 relationships among them are still largely unknown.

85 SasG, also known as Aap in *Staphylococcus epidermidis*, is one of the
86 extensively characterized CWAPs in *S. aureus* and promotes cell-cell interactions during
87 biofilm formation (29, 30). SasG/Aap is comprised of the N-terminal secretion signal, the
88 A domain, and the repeated B domains harboring two short G5-E repeats, followed by the
89 C-terminal wall/membrane-spanning regions containing the LPXTG motif (31). Biofilm
90 promotion is mainly achieved by interactions between B domains of two SasG/Aap
91 molecules in a Zn²⁺-dependent fashion (32). Atomic force microscopy demonstrated that
92 homophilic interactions between B domains of two SasG/Aap molecules are involved in

93 biofilm promotion activity (33). On the other hand, it is still unclear whether cell
94 wall-anchorage is essential for the SasG/Aap function in biofilm promotion.

95 In the current study, we aimed to define the roles of Eap and SasG in biofilm
96 formation. We show that the secreted protein Eap and CWAP SasG compensate for one
97 another in biofilm formation, but only Eap plays a key role in the ruggedness of biofilm
98 structure. In addition, loss of both proteins significantly reduces the pathogenicity of *S.*
99 *aureus* in a silkworm larval infection model. These findings provide insight into the
100 multicellular behaviors and pathogenicity of *S. aureus* and emphasize the importance of
101 developing anti-biofilm therapies that target multiple biofilm components.

102 **RESULTS**

103 **Eap and CWAPs play similar roles in biofilm biomass determination.** In the
104 current study, *S. aureus* strains were cultured at 37°C in brain heart infusion (BHI)
105 medium supplemented with 1% (w/v) glucose (BHIG medium), since a large variety of *S.*
106 *aureus* strains produce substantial biofilms under these conditions (34). We previously
107 showed that MR23, a clinical methicillin-resistant isolate of *S. aureus*, forms a robust
108 protein-dependent biofilm in BHIG that is dispersed by proteinase K (Fig. S1) (35). To
109 identify proteins that are important for biofilm formation, known biofilm-associated genes
110 were deleted in MR23 by using the in-frame deletion method (36, 37). Although MR23
111 ECM contains large amounts of Eap and Eap promotes biofilm formation in strains that
112 do not produce substantial biofilms (35), deletion of *eap* did not affect the biomass of
113 MR23 biofilm (Fig. 1A), similarly to *S. aureus* SA113 Δeap grown in BHIG (25). This
114 suggested that Eap does not contribute to biofilm formation in MR23 and/or that other
115 molecules, including proteins, eDNA, and PIA, compensate for the loss of Eap function.
116 To address the latter possibility, we treated a preformed MR23 Δeap biofilm with enzymes
117 that degrade major biofilm components. The biofilm was destroyed by proteinase K, but
118 not by DNase I or PIA-degrading dispersin B (Fig. S1A). This indicated that MR23 Δeap
119 formed a protein-dependent biofilm and that other proteins contributed to biofilm

120 formation.

121 CWAPs are important for biofilm formation in various bacteria (38–42). We
122 therefore asked whether CWAPs play a role in biofilm formation in MR23 Δeap . Sortase A
123 covalently links the CWAP LPXTG motif to peptidoglycan, anchoring CWAPs to the cell
124 wall (27). Therefore, the role of cell wall-anchored CWAPs can be investigated by
125 deleting *srtA*. To test whether Eap played a role in biofilm formation, *srtA* was disrupted in
126 MR23 wild-type and MR23 Δeap . Although the biofilm biomass of the $\Delta srtA$ mutant was
127 the same as that of the wild type, strain $\Delta eap \Delta srtA$ formed significantly less biofilm than
128 other strains (Fig. 1A). In addition, the biomass of $\Delta eap \Delta srtA$ strain biofilm was restored
129 by expressing either Eap or SrtA from the respective plasmids (Fig. 1B). Expression of
130 Eap and SrtA was confirmed by sodium dodecyl sulfate-polyacrylamide gel
131 electrophoresis (SDS-PAGE) of ECM (Fig. 1C) and cell wall fractions (Fig. 1D).
132 Drastically reduced levels of CWAPs in $\Delta eap \Delta srtA$ mutant were recovered by the
133 expression of exogenous SrtA (Fig. 1D). These observations indicated that Eap and
134 certain cell wall-anchored CWAP(s) play redundant roles in the formation of the
135 substantial protein-dependent biofilm of MR23.

136 **Eap and SasG play redundant roles in biofilm formation.** To identify the
137 CWAP that compensated for the loss of Eap in biofilm formation by MR23, we disrupted

138 major CWAP-encoding genes belonging to different groups (26) in MR23 wild type and
139 Δeap mutant. Simultaneous deletion of *eap* and *sasG* resulted in a significant reduction
140 of the biofilm biomass, while combined deletions of *eap* and other CWAP genes did not
141 (Fig. 2A). In addition, the biomass of $\Delta sasG$ mutant biofilm was similar to those of
142 wild-type and Δeap strains (Fig. 2A). The reduced biomass of $\Delta eap \Delta sasG$ strain biofilm
143 was restored by the expression of either Eap or SasG from the respective plasmids (Fig.
144 2B). Expression of Eap and SasG was confirmed by SDS-PAGE (Fig. 2C) and western
145 blotting (Fig. 2D). Of note, the amount of SasG produced by a plasmid-encoded gene
146 was higher than that of wild-type strain harboring the empty vector pLC1 (Fig. 2D), which
147 may account for a slight increase in biomass of biofilm formed by $\Delta eap \Delta sasG$ mutant
148 harboring pSasG^{WT} (Fig. 2B). These observations revealed that Eap and SasG play
149 redundant roles in the formation of substantial biofilm by MR23.

150 MR23 is a hyper Eap-producing strain compared with other clinical isolates as
151 recently reported (34). In addition, the protein level of SasG in MR23 was similar or
152 higher than those in most other strains (Fig. S2). Therefore, the redundant roles of Eap
153 and SasG might be specific for certain strains that overproduce Eap and SasG. As shown
154 in Fig. S3A, single knockouts of *eap* and *sasG* slightly reduced the biofilm biomass in
155 RN4220, a restriction-deficient strain of *S. aureus* derived from the laboratory strain

156 NCTC8325 (43), while double knockout of both genes did so more effectively.
157 Overproduction of either Eap or SasG drastically stimulated biofilm formation of RN4220
158 $\Delta eap \Delta sasG$. The biofilm biomass of RN4220 $\Delta eap \Delta sasG$ co-overexpressing Eap and
159 SasG was similar to those of cells overexpressing each protein (Fig. S3B). Under the
160 conditions tested, the amount of Eap expressed from pEap-SasG was lower than that
161 from pEap, while the amount of SasG produced from pEap-SasG was almost the same
162 as that from pSasG (Fig. S3C). Supplementation of high concentrations of
163 anhydrotetracycline (aTc), an inducer, did not stimulate biofilm formation of RN4220 Δeap
164 $\Delta sasG$ pEap-SasG (data not shown). Therefore, we added purified Eap into the biofilm
165 culture of RN4220 $\Delta eap \Delta sasG$ pEap-SasG. Exogenously added Eap did not promote
166 biofilm formation of RN4220 $\Delta eap \Delta sasG$ pEap-SasG, although it stimulated that of
167 RN4220 $\Delta eap \Delta sasG$ pLC1 in a dose-dependent manner (Fig. S3D). Analysis of
168 extracellular matrix confirmed that a sufficient amount of Eap was used in this experiment,
169 since Eap in the culture of RN4220 $\Delta eap \Delta sasG$ pEap was estimated to be 90.9 ± 2.9 nM
170 ($n = 3$). These results indicate that redundancy between Eap and SasG is likely specific
171 for certain strains that overproduce Eap and SasG as in the case of MR23.

172 **SasG is a DNA-binding protein and capable of stabilizing eDNA in the**
173 **biofilm.** The biofilms formed by wild type and Δeap were resistant to DNase I-treatment,

174 whereas those by $\Delta sasG$ and $\Delta eap \Delta sasG$ were sensitive slightly and remarkably,
175 respectively (Figs. 3A and S1), suggesting two possibilities that Eap and SasG interact
176 with and protect eDNA from nucleases and that the importance of eDNA is masked by
177 these proteins. Recently, it has been reported that Eap can bind to DNA and is capable of
178 blocking neutrophil extracellular trap (NETs) formation (44). However, DNA-binding
179 capacity of SasG has not yet been elucidated. Therefore, we performed gel shift assay to
180 examine the interaction between SasG and DNA. As shown in Figure 3B, purified SasG
181 bound to purified lambda DNA in a dose-dependent manner. Next, we examined effect of
182 SasG on the stability of DNA. Although lambda DNA was digested by DNase I rapidly,
183 SasG protected it from degradation under the tested conditions (Fig. 3C). Taken together,
184 these results indicate that SasG is a DNA-binding protein and capable of stabilizing
185 eDNA in the biofilm.

186 **Cell wall-anchorage of SasG is essential for biofilm formation.** SasG
187 contains an N-terminal signal peptide, A domain, repeated B domains, and LPXTG motif
188 (28). DNA sequencing revealed that the MR23 *sasG* gene encodes a protein of
189 approximately 108 kDa, containing four B domains (Figs. 4A and S4). SasG promotes
190 adhesion of bacterial cells during biofilm formation, and while interactions between the B
191 domains are important for adhesion, the A domain is dispensable (31). However, it was

192 unclear whether cell wall-anchorage was essential for SasG function in biofilm
193 development. To address this, we removed the SasG LPXTG motif and tested whether
194 that affected biofilm formation by MR23. Plasmid-encoded wild-type SasG (SasG^{WT})
195 restored the biofilm biomass of $\Delta eap \Delta sasG$ strain to wild-type levels, whereas
196 expression of the protein lacking the LPXTG motif (SasG^{ΔL}) did not (Fig. 4B). As
197 expected, SasG^{WT} was present in the cell wall fraction but SasG^{ΔL} was not (Fig. 4C). By
198 contrast, large amount of SasG^{ΔL} was detected in the culture supernatant (Fig. 4D).
199 These observations indicated that cell wall-anchorage is essential for the key role of
200 SasG in biofilm formation. This was consistent with the reduced biofilm biomass of Δeap
201 $\Delta srtA$ strain (Fig. 1A), in which SasG was not tethered to the cell wall.

202 **Eap plays an important role in rugged biofilm formation.** Eap is a major
203 component of MR23 ECM. Eap contributes to biofilm formation by promoting bacterial
204 cohesion and bacterial cell-surface interactions (30, 38), whereas SasG promotes
205 bacterial cell-cell adhesion (31). To determine whether these proteins affected the
206 three-dimensional structure of MR23 biofilm, we analyzed biofilms formed by MR23
207 wild-type and derived mutant strains by using confocal laser scanning microscopy
208 (CLSM). Wild-type strain formed a thick biofilm with a highly rugged surface (Fig. 5).
209 Strain $\Delta sasG$ formed a biofilm whose thickness and ruggedness were similar to those of

210 the wild-type biofilm. Strain Δeap formed a biofilm with a similar thickness but smoother
211 than those of wild-type and $\Delta sasG$ strain biofilms. On the other hand, strain $\Delta eap \Delta sasG$
212 formed a thin and smooth biofilm. These observations indicated that Eap and SasG play
213 similar roles in determining biofilm biomass and thickness, but different roles in
214 determining biofilm ruggedness.

215 We then analyzed biofilms at an initial phase of formation (4-h biofilms) by using
216 atmospheric scanning electron microscopy (ASEM). This enabled the visualization of
217 biofilms in solution at a higher resolution than that afforded by CLSM, and with minimal
218 artifacts caused by dehydration (45). MR23 wild-type biofilm contained highly aggregated
219 cell clusters (Fig. S4). By contrast, biofilm formed by strain $\Delta eap \Delta sasG$ spread on the
220 surface of ASEM dish, and the formed cell clusters were smaller and less numerous than
221 those of wild-type strain. In addition, both focused and defocused cells were observed in
222 wild-type strain, while focused cells were predominant in strain $\Delta eap \Delta sasG$. This
223 indicated that the former formed a multilayer biofilm while the latter formed a monolayer
224 biofilm after 4-h cultivation. These differences might be associated with the
225 three-dimensional structures of the biofilms observed using CLSM (Fig. 5).

226 **Double deletion of *eap* and *sasG* reduces pathogenicity of *S. aureus*.** We
227 next examined the impact of *eap* and *sasG* deletion on the pathogenicity of *S. aureus in*

228 *vivo*, using the silkworm larvae (*Bombyx mori*) as a model of human pathogenic bacterial
229 infection (46). All silkworm larvae survived for at least 60 h after injection of 0.6% NaCl
230 solution, but 70% of larvae died within that period after injection of 1×10^7 cells of MR23
231 wild type (Fig. 6). No statistically significant difference in the survival rate of silkworm
232 larvae infected with Δeap strain and wild type were apparent. Similarly, no statistically
233 significant differences were observed in the mortality of larvae infected with $\Delta sasG$ and
234 wild-type strains. By contrast, the survival rate of silkworm larvae infected with Δeap
235 $\Delta sasG$ strain was significantly higher than that of larvae infected with the wild type (Fig.
236 6). Since proliferation of *S. aureus* in silkworm larvae is required for the lethality of
237 infection (46), we also evaluated the survival of the tested strains in silkworm larvae. After
238 24-h infection, no significant differences in the retrieved CFU/ml were apparent between
239 the strains (Fig. S5). Since the mortality of larvae infected with $\Delta eap \Delta sasG$ was
240 significantly lower than that of larvae infected with the wild type, this indicated that the
241 effect was not associated with a reduction of bacterial cell numbers in silkworm larvae,
242 but rather, with the strain's biofilm forming capacity *in vitro*.

243

244 DISCUSSION

245 In the current study, genetic and microscopic analyses, and silkworm infection

246 experiments revealed that the secreted protein Eap and CWAP SasG play redundant and
247 distinct roles in biofilm development and pathogenicity of *S. aureus*. To the best of our
248 knowledge, this is the first-ever report describing the functional relationship between a
249 secreted protein and a bona fide cell wall-anchored CWAP in the multicellular behavior
250 and pathogenesis of an opportunistic pathogen.

251 Mutational analyses revealed that simultaneous disruption of *eap* and *srtA*, and
252 that of *eap* and *sasG* resulted in a significant reduction of the biomass of MR23 biofilm
253 (Figs. 1 and 2). However, the biomass of $\Delta eap \Delta srtA$ strain biofilm was lower than that of
254 $\Delta eap \Delta sasG$ strain biofilm (Figs. 1 and 2), indicating that additional CWAP(s) might be
255 responsible for biofilm formation by the $\Delta eap \Delta sasG$ strain. In addition, strain $\Delta eap \Delta srtA$
256 formed a low but significant amount of biofilm (approximately 25% of that produced by
257 the wild type) that was sensitive to proteinase K and DNase I, but not dispersin B (Fig.
258 S1), suggesting that other non-CWAP proteins and eDNA contribute slightly to biofilm
259 formation.

260 SasG promotes cell-cell interactions during biofilm formation. This is mainly
261 achieved by interactions between B domains of two SasG molecules anchored to
262 different *S. aureus* cells, in a Zn^{2+} -dependent fashion (32). Although at least five B
263 domains were shown to be indispensable for SasG to promote biofilm formation, the

264 number of B domain varies between 2 and 10 (29). In the current study, we confirmed
265 that MR23 SasG harbors four B domains (Accession number: LC388387) and yet it
266 contributes to biofilm formation of MR23 (Fig. 1). The slight contradiction between the
267 previous study and our study regarding the number of B repeats required for biofilm
268 formation could be due to the different strains and experimental conditions. Eap harbors
269 four to six tandem repeats of a characteristic domain, the EAP domain, comprised of an
270 alpha-helix positioned diagonally across a five-stranded, mixed beta-sheet (47). DNA
271 sequencing revealed that MR23 Eap has five EAP domains (Accession number:
272 LC388386). Revisiting the minimum number of B domains in SasG and determining the
273 role of EAP domain in biofilm formation will provide further insights into molecular
274 mechanisms of biofilm formation mediated by these proteins.

275 Previously, the involvement of a secreted protein Sbp and a cell wall-anchored
276 protein Aap in biofilm formation was analyzed in *S. epidermidis* (48). The authors
277 reported that Sbp, but not Aap, is involved in biofilm formation of *S. epidermidis* strain
278 1457, a PIA-dependent biofilm producer. They noticed that reduced biofilm formation in
279 Δsbp was due to the down regulation of *icaA* transcription. Subsequently, the authors
280 revisited the roles of Sbp and Aap in an *ica*-negative mutant of strain 1457.
281 Overproduction of the B domains of Aap and supplementation of recombinant Sbp

282 promoted biofilm formation of the *ica*-negative strain in a dose-dependent manner. It
283 should be emphasized that the authors used only the B domain of Aap (amino acids
284 596-1507) that was not covalently linked to the cell wall and did not show the importance
285 of cell wall-anchored Aap. Interestingly, we found that cell wall-anchorage was essential
286 for SasG function in MR23 biofilm and that the role of SasG was reinforced in the
287 absence of Eap (Fig. 4). On the other hand, *S. aureus* protein A and *Listeria*
288 *monocytogenes* internalin A do not require cell wall-anchoring to promote biofilm
289 development (39, 49). The requirement of cell wall-anchorage for biofilm promotion
290 depends on the CWAP. Protein A and internalin A may bind to cell surface even in the
291 absence of the LPXTG motif and are expected to promote bacterial cell-cell interactions
292 via protein-protein or protein-other component(s) interactions. Data presented herein
293 indicated that SasG^{AL} was present in the culture supernatant but no or very little protein
294 was present in the cell surface fraction (Fig. 4). This suggested that SasG was unable to
295 associate tightly with the bacterial cell surface in the absence of the LPXTG motif.
296 Reduced biofilm formation by strain $\Delta eap \Delta srtA$ (Fig. 1) supported this notion, since
297 LPTXG-containing proteins cannot be covalently bridged to the cell wall in that strain.

298 CLSM analysis revealed that Δeap and $\Delta sasG$ strains produced a thick biofilm,
299 similar to the wild type, and that strain $\Delta eap \Delta sasG$ formed a thinner biofilm than the wild

300 type (Fig. 5). These observations were consistent with the results of conventional crystal
301 violet staining (Fig. 2A). Interestingly, deletion of *eap* significantly reduced the
302 ruggedness of the MR23 biofilm, whereas that of *sasG* did not (Fig. 5), indicating that
303 Eap contributes to the ruggedness of the biofilm. ASEM analysis indicated that Eap is
304 important for bacterial cohesion, leading to the formation of highly aggregated cell
305 clusters at the initial stage of biofilm formation (Fig. S4). This property of Eap appeared to
306 be associated with the roughness of biofilm.

307 We also examined the impact of *eap* and *sasG* deletions on *S. aureus*
308 pathogenicity *in vivo*, using the silkworm larva model. No statistically significant
309 differences between the survival rates of silkworm larvae infected with wild-type and
310 Δeap strains were apparent; however, the survival rate of silkworm larvae infected with
311 Δeap strain was slightly higher than that of larvae infected with wild-type and $\Delta sasG$
312 strains (Fig. 6). Eap contributes to the virulence of *S. aureus* by interacting with bacterial
313 cell surface and several host plasma proteins (22, 23). The role of SasG in virulence is
314 still unclear. It was reasonable to assume that the effect of Eap on pathogenicity is
315 greater than that of SasG, and that biofilm biomass quantified *in vitro* correlated with
316 pathogenicity. Indeed, the pathogenicity of *S. aureus* in the silkworm larva model is
317 associated with adhesion to host cells but not toxin production (50). Therefore, it is not

318 surprising that key players in biofilm formation also contribute to pathogenicity in
319 silkworm larvae.

320 How does MR23 produce the large amount of Eap and SasG and how does such
321 strain emerge? Our preliminary data revealed that *agrC* and one-third of *agrA* are
322 spontaneously deleted in MR23 (data not shown). Dysfunction of *agr* leads to
323 up-regulation of the expression of surface proteins including Spa and FnBA at the
324 transcriptional (51–53) and protein levels (54, 55). Although regulation of SasG
325 expression is largely unknown, a previous report suggested that the transcription of *sasG*
326 was increased in *agr*-dysfunctional isolates (56). In addition, surface proteins are
327 stabilized due to down regulation of the expression of extracellular proteases in *agr*
328 mutants (57). These data suggest that *agr* dysfunction may be involved in the enhanced
329 expression and accumulation of SasG in MR23. Previously, it was reported that *S.*
330 *aureus* Newman produced a high amount of Eap via enhanced activity of SaeS, a
331 positive regulator of Eap, due to a unique mutation in SaeS (Leu18 to Pro18) (58). The
332 same mutation was not found in MR23, but another mutation was detected in the
333 C-terminal part of SaeS (Val299 to Leu299). It would be interesting to determine whether
334 the latter mutation is also involved in the overproduction of Eap. Glucose was shown to
335 repress SaeS, leading to down regulation of Eap (59); however, MR23 still produced a

336 large amount of Eap even in the presence of glucose (34). Therefore, other factors, apart
337 from SaeS, should also be involved in the extremely high amount of Eap in MR23. We
338 found a single-base substitution in the 5'-untranslated region of *eap* in MR23 compared
339 with other strains (data not shown). This base-substitution may stabilize *eap* mRNA
340 and/or promote its translation, which could account for the extremely high amount of Eap
341 in MR23.

342 Taken together, the presented findings highlight the functional relationship
343 between a secreted protein and a CWAP in *S. aureus* biofilm formation and pathogenicity.
344 There may be similar redundancies between Eap and SasG, between other secretion
345 protein(s) and other CWAP(s), between proteins and eDNA, and between
346 polysaccharides and other extracellular substances in other strains and bacteria. In fact,
347 we found redundancy between proteins (Eap and SasG) and eDNA, as the DNase
348 I-resistant biofilm of MR23 became DNase I-sensitive when *eap* and *sasG* were deleted
349 (Figs. 3A and S1). In addition, our results indicate for the first time that SasG binds to and
350 stabilizes DNA (Fig. 3B, C). The present paper will provide an important avenue to
351 consider that different biofilm adhesins may play overlapping roles in both biofilm
352 formation and infection. This knowledge may contribute to the development of anti-biofilm
353 therapies targeting multiple biofilm components.

354 **METHODS**

355 **Bacterial strains and culture media.** Bacterial strains used in the current study
356 are listed in Table S1. *S. aureus* strains were grown at 37°C in BHI medium (Becton
357 Dickinson, Franklin lakes, NJ), BHIG medium (Wako, Osaka, Japan), or mannitol salt
358 agar (Merck, Darmstadt, Germany). *Escherichia coli* strains were grown at 37°C in
359 Luria-Bertani (LB) medium containing 1% (w/v) tryptone (Becton Dickinson), 0.5% (w/v)
360 yeast extract (Becton Dickinson), and 1% (w/v) NaCl. When required, appropriate
361 antibiotics (100 µg/ml ampicillin and 5 µg/ml chloramphenicol; Nacalai Tesque, Kyoto,
362 Japan) and an inducer (100 ng/ml aTc; Sigma, St. Louis, MO) were added to the media.

363 **Plasmid construction.** Mutant strains of *S. aureus* MR23 were constructed
364 using the *E. coli*-*S. aureus* shuttle vector pKOR1 (37) as described by Chiba *et al.* (60).
365 Briefly, sequences approximately 500-bp upstream and downstream of each target gene
366 were PCR-amplified from MR23 genomic DNA using KOD Plus ver. 2 DNA polymerase
367 (Toyobo, Osaka, Japan) and the appropriate primer sets (Table S2). The fragments were
368 connected by splicing using overlap extension PCR (36). The generated PCR products
369 were cloned into pKOR1 using the Gateway BP Clonase II enzyme mix (Life
370 Technologies, Palo Alto, CA); the resulting plasmids are described in Table S2.

371 Plasmids for the complementation of the respective gene deletions were

372 constructed using the *E. coli*–*S. aureus* shuttle vector pLC1 as previously described (61).
373 Briefly, *eap*, *srtA*, *sasG^{WT}*, *sasG^{ΔL}*, and *eap-sasG^{WT}* genes were PCR-amplified from
374 genomic DNA using KOD Plus ver. 2 DNA polymerase and primers listed in Table S2.
375 The amplified fragments were cloned into pLC1 linearized by inverse PCR with primers
376 pLC1-F and pLC1-R (Table S2) using the GeneArt Seamless cloning and assembly kit
377 (Life Technologies) according to the manufacturer's instructions.

378 To overproduce recombinant N-terminally His₆-tagged SasG (His-SasG) in *E. coli*,
379 the fragment encoding MR23 SasG lacking the signal sequence and the C-terminal
380 portion with the LPXTG motif (amino acid residues 51–954) was PCR-amplified from the
381 MR23 genome using KOD Plus Neo DNA polymerase (Toyobo), and the primers
382 pCold-SasG-F and pCold-SasG-R (Table S2). The amplified fragment was cloned into
383 pCold I (Takara, Otsu, Japan) using the GeneArt Seamless cloning and assembly kit, as
384 above. The resultant plasmid was named pCold-SasG (Table S1).

385 Oligonucleotide primers (Table S2) were synthesized by Life Technologies.

386 **Construction of deletion mutants.** Plasmids derived from pKOR1, described
387 above, were used to transform *S. aureus* RN4220 by electroporation (62). After
388 purification, the plasmids were introduced into strain MR23 by electroporation, and the
389 target genes were deleted from the MR23 genome by in-frame deletion as described

390 previously (32, 45) (Table S1). Similarly, RN4220 isogenic mutants were generated.

391 **Biofilm formation.** Overnight *S. aureus* cultures grown in BHI medium at 37°C
392 were diluted 1000 times in BHIG. Then, 200- μ l suspensions were cultured at 37°C for 24
393 h in 96-well polystyrene flat-bottom plates (Corning, Corning, NY). When required, aTc
394 (100 ng/ml), an inducer, and chloramphenicol (5 μ g/ml), a selective agent, were added to
395 the culture medium from the onset of biofilm formation. Biofilms formed on plastic surface
396 were washed twice with 200 μ l of phosphate-buffered saline and stained with 200 μ l of
397 0.05% (w/v) crystal violet for 5 min at 25°C. After staining, biofilms were washed once
398 with 200 μ l of phosphate-buffered saline and their mass quantified by measuring the
399 absorbance at 595 nm using a microplate reader Infinite F200 Pro (Tecan, Männedorf,
400 Switzerland). The limit of the microplate reader was $ABS_{595} = 4.0$.

401 To analyze the biofilm susceptibility to enzymes, proteinase K (100 μ g/ml)
402 (Sigma), DNase I (100 U/ml) (Roche, Mannheim, Germany), or dispersin B (20 μ g/ml)
403 (Kane Biotech, Winnipeg, MB, Canada) (63) were added to 24-h biofilms and incubated
404 for 1 h at 37°C. Biofilm biomass was then quantified as described above.

405 **Isolation of ECM, cell wall, and culture supernatant fractions.** ECM was
406 isolated from bacteria grown under biofilm-forming conditions as previously reported (60).
407 Briefly, overnight cultures were diluted 1000 times in 10 ml of BHIG medium in 15-ml

408 conical tubes (Becton Dickinson) and statically incubated at 37°C for 24 h. After
409 incubation, the conical tubes were centrifuged at 8000 × *g* for 10 min at 25°C to separate
410 bacterial cells from culture supernatant. To extract ECM components, cell pellets were
411 suspended in 100 μl of 1.5 M NaCl solution. The suspensions were centrifuged at 5000 ×
412 *g* for 10 min at 25°C. The supernatants (ECM fractions) were then transferred to new test
413 tubes. Cell pellets were suspended in 100 μl of 25% (w/v) sucrose (Nacalai Tesque)
414 solution containing 10 mM Tris-HCl (pH 8.0) (Wako) and protease inhibitor cocktail
415 (Nacalai Tesque). The suspensions were treated with lysostaphin (200 μg/ml) (Wako) for
416 30 min at 37°C and then centrifuged at 15,000 × *g* for 10 min at 25°C. The supernatants
417 were collected as the cell wall fractions. To concentrate the culture supernatants, the
418 supernatants (600 μl) were mixed with equal amount of 20% (w/v) trichloroacetic acid
419 (Nacalai Tesque) and incubated for 30 min on ice. After centrifugation at 10,000 × *g* for 10
420 min at 4°C, the pellets were washed with 1 ml of acetone (Wako) and centrifuged (10,000
421 × *g* for 10 min at 4°C). The pellets were suspended in 60 μl of SDS sample buffer [125
422 mM Tris-HCl (pH 6.8), 4% (w/v) SDS, 20% (w/v) glycerol, 10% (v/v) 2-mercaptoethanol]
423 and used as concentrated (10×) culture supernatant fractions.

424 **Purification of recombinant SasG.** His-SasG was overexpressed from
425 pCold-SasG in *E. coli* BLR (DE3) cells (Table S1), which were grown at 30°C in 1 l of LB

426 medium containing 100 µg/mL ampicillin. Expression of His-SasG was induced by the
427 addition of isopropyl β-D-1-thiogalactopyranoside (1 mM) and incubating at 15°C for 24 h.
428 Cells were harvested by centrifugation and resuspended in 50 ml of buffer A [20 mM
429 Tris-HCl (pH 8.0) and 300 mM NaCl] supplemented with protease inhibitor cocktail
430 (Nacalai Tesque). After sonication on ice, cell lysates were centrifuged at 8500 × *g* for 30
431 min at 4°C, and the supernatant was loaded onto 2-ml bed volume of TALON resin
432 (Takara) that had been washed with buffer A supplemented with 5 mM imidazole.
433 Recombinant proteins were eluted using 250 mM imidazole. Eluted fractions were
434 dialyzed against buffer B [20 mM Tris-HCl (pH 8.0), 1 mM dithiothreitol, and 20% (w/v)
435 glycerol] using Slide-A-Lyzer dialysis cassettes (Thermo Fisher, Waltham, MA), and
436 purified by chromatography using a HiTrap Q column (GE Healthcare, Pittsburgh, PA)
437 and 0–1 M NaCl gradient in buffer C [20 mM Tris-HCl (pH 8.0), 1 mM dithiothreitol, and
438 10% (w/v) glycerol]. Purified His-SasG was pooled and quantified using Bradford assay
439 kit (Bio-Rad Laboratories, Hercules, CA).

440 **Characterization of proteins in ECM, cell wall, and culture supernatant**
441 **fractions.** The amount of proteins in the ECM fractions was standardized to the wet
442 weight of bacterial pellets before ECM fraction isolation. Protein concentrations in the cell
443 wall fractions were determined using Pierce protein assay reagent (Thermo Fisher).

444 Standardized amounts of proteins were resolved on 15% (w/v) polyacrylamide gels (Atto,
445 Tokyo, Japan). After SDS-PAGE, the gels were stained with CBB (Nacalai Tesque) or
446 used for western blotting.

447 **Western blotting.** After SDS-PAGE, proteins were transferred to a
448 polyvinylidene difluoride membrane using iBlot 2 dry blotting system (Thermo Fisher).
449 The membrane was treated for 30 min at 25°C with 1% (w/v) skimmed milk (Wako)
450 dissolved in Tris-buffered saline (TBS-T) composed of 10 mM Tris-HCl (pH 7.4) (Wako),
451 100 mM NaCl, and 0.1% (v/v) Tween 20. After gentle washing with TBS-T, the membrane
452 was probed with anti-SasG primary rabbit polyclonal antibody [developed by Eurofins
453 Genomics (Tokyo, Japan) using purified His-SasG as the antigen] diluted 5000 times in
454 CanGet Signal 1 (Toyobo), for 1 h at 25°C. The membrane was washed twice with TBS-T
455 and was subsequently incubated with a secondary goat anti-rabbit IgG antibody
456 conjugated with horse radish peroxidase (BioRad Laboratories) diluted 100,000 times in
457 CanGet Signal 2 (Toyobo), for 1 h at 25°C. After washing three times with TBS-T, the
458 signal was detected using ECL prime western blotting detection reagent (GE Healthcare)
459 and LAS-4000 Image Analyzer (GE Healthcare).

460 **Gel shift assay.** Purified SasG (0.1, 0.5, and 1 μ M) was mixed with purified
461 lambda DNA (15 μ g/ml, Takara) in buffer containing 0.5 mM Tris-HCl (pH 8.0) and 0.05

462 mM EDTA. After incubation at 25°C for 1 h, the samples were analyzed by agarose gel
463 electrophoresis with ethidium bromide staining.

464 **DNA protection assay.** Purified lambda DNA (15 µg/ml, Takara) was
465 pre-incubated with or without purified SasG (1 µM) in buffer containing 400 mM Tris-HCl
466 (pH 7.9), 100 mM NaCl, 60 mM MgCl₂, and 10 mM CaCl₂ at 25°C for 30 min. Then,
467 DNase I (1 U/ml) was added to the mixture. At the indicated time points, small aliquots of
468 the mixture were taken, mixed with proteinase K (1 mg/ml), and incubated at 25°C for 10
469 min to digest DNase I and SasG. The residual DNA was analyzed by agarose gel
470 electrophoresis. Band intensities were measured using LAS-4000 Image Analyzer.

471 **CLSM.** Overnight bacterial cultures grown in BHI medium at 37°C were diluted
472 1000 times in BHIG and incubated at 37°C for 24 h on glass-bottomed dish (35-mm
473 diameter; Matsunami Glass, Osaka, Japan). Biofilms were fixed with 1% (w/v)
474 glutaraldehyde for 10 min at 25°C (Wako). After glutaraldehyde removal, 50 mM
475 ammonium chloride (Kanto Chemical, Tokyo, Japan) was added to quench the residual
476 glutaraldehyde. The fixed biofilms were stained with 25 µM of thioflavin T (AAT Bioquest,
477 Sunnyvale, CA), which binds to bacterial RNA and is used to visualize bacterial cells (64).
478 Three-dimensional biofilm structures were observed using LSM880 confocal laser
479 scanning microscope with a 63× oil objective lens (Carl Zeiss, Oberkochen, Germany).

480 Thioflavin T fluorescence was detected using excitation at 458 nm and emission at 470–
481 510 nm. All z-sections were collected at 0.25- μ m intervals and three-dimensional
482 structures were reconstructed using the free microscope software ZEN for ZEISS
483 Microscopy (Carl Zeiss).

484 **Evaluation of *S. aureus* pathogenicity in the silkworm model.** Fifth instar
485 silkworm larvae of *B. mori* (S30 \times xe5) were obtained from the Institute of Genetic
486 Resources Faculty of Agriculture (Kyusyu University, Fukuoka, Japan). To prepare
487 bacterial suspensions, 700 μ l of overnight cultures were centrifuged at 8000 \times *g* for 5 min
488 at 25°C. The pellets were washed with 700 μ l of 0.6% NaCl solution, centrifuged at 8000
489 \times *g* for 5 min at 25°C, and re-suspended in 700 μ l of 0.6% NaCl solution. Then, 50 μ l of
490 bacterial suspensions were injected (1×10^7 CFU) into the hemolymph through the dorsal
491 vessel using 30-G syringe (Becton Dickinson). Pressure was immediately applied to the
492 injection site for 20 s to stop leakage of the body fluid. As a control, larvae were injected
493 with 50 μ l of 0.6% NaCl solution. Larval survival was observed at 25°C for 60 h without
494 feeding.

495 To evaluate bacterial survival in silkworm larvae, the rear legs of injected
496 silkworms were cut with scissors and the body fluid was collected, 24 h after injection of
497 bacteria. After 10-fold serial dilution, samples were spread on mannitol salt agar plates

498 selective for *S. aureus*, incubated at 37°C overnight, and the colonies counted.

499 **Accession numbers.** Nucleotide sequences of *eap* and *sasG* from *S. aureus*
500 MR23 determined in the current study have been deposited in the DDBJ database under
501 the accession numbers LC388386 and LC388387, respectively.

502 **Statistical analyses.** Statistical analysis of biofilm biomass was performed using
503 EZR software (57). ANOVA and Student's *t*-test were used to assess significant
504 differences in biofilm formation between bacterial strains and in enzyme susceptibility
505 between treatments. For multiple group comparisons, Kruskal-Wallis and Mann-Whitney
506 U-tests with Bonferroni correction were used to determine whether any of the groups
507 exhibited statistically significant different thickness of biofilms. The log-rank test was
508 used to assess significant differences in the pathogenicity of bacterial strains in the
509 silkworm model. For all statistical analyses, $P < 0.05$ was considered significant.

510 **Acknowledgements**

511 The authors acknowledge Dr. Bae for providing pKOR1; Dr. Cui for gifting pLC1; Ms.
512 Anne-Aurelie Lopes for critical reading of the manuscript; and all members of the
513 Department of Bacteriology in Jikei University for stimulating discussions. This work was
514 in part supported by a Grant-in-Aid for Young Scientists (A) from JSPS (no. 15H05619 to
515 S.S.); a Grant-in-Aid for Scientific Research (B) from JSPS (no. 26293100 to Y.M.); a
516 grant from the MEXT-Supported Program for the Strategic Research Foundation at
517 Private Universities, 2012–2016 (to Y.M.); and JST ERATO (no. JPMJER1502 to S.S.).

518 The authors declare no conflict of interests.

519

520 **Author contributions**

521 A.C., S.S., and Y.M. planned the project. K.Y., A.C., and S.S. designed the experiments
522 K.Y., A.C., and S.S. performed the experiments and analyzed the data. C.S. developed
523 Nanogold- and heavy metal-labeling for biofilms and assisted during ASEM analysis. K.Y.,
524 A.C., and S.S. wrote the paper with input from M.S., Y.K., K.M., and Y.M.

525 **References**

- 526 1. Flemming H-C, Neu TR, Wozniak DJ. 2007. The EPS Matrix: The “House of Biofilm
527 Cells.” J Bacteriol 189:7945–7947.
- 528 2. Hall-Stoodley L, Costerton JW, Stoodley P. 2004. Bacterial biofilms: from the
529 Natural environment to infectious diseases. Nat Rev Microbiol 2:95–108.
- 530 3. Costerton JW. 1999. Bacterial Biofilms: A Common Cause of Persistent Infections.
531 Science (80-) 284:1318–1322.
- 532 4. Lebeaux D, Ghigo J-M, Beloin C. 2014. Biofilm-Related Infections: Bridging the
533 Gap between Clinical Management and Fundamental Aspects of Recalcitrance
534 toward Antibiotics. Microbiol Mol Biol Rev 78:510–543.
- 535 5. Mah T-FC, O’Toole GA. 2001. Mechanisms of biofilm resistance to antimicrobial
536 agents. Trends Microbiol 9:34–39.
- 537 6. Römling U, Balsalobre C. 2012. Biofilm infections, their resilience to therapy and
538 innovative treatment strategies. J Intern Med 272:541–561.
- 539 7. Kluytmans J, Belkum A van, Verbrugh H. 1997. Nasal Carriage of *Staphylococcus*
540 *aureus*: Epidemiology, Underlying Mechanisms, and Associated Risks. Clin
541 Microbiol Rev 10:505–520.
- 542 8. Wertheim HF, Melles DC, Vos MC, van Leeuwen W, van Belkum A, Verbrugh H a,
543 Nouwen JL. 2005. The role of nasal carriage in *Staphylococcus aureus* infections.
544 Lancet Infect Dis 5:751–762.
- 545 9. Arciola CR, Campoccia D, Speziale P, Montanaro L, Costerton JW. 2012. Biofilm

- 546 formation in *Staphylococcus* implant infections. A review of molecular mechanisms
547 and implications for biofilm-resistant materials. *Biomaterials* 33:5967–5982.
- 548 10. Tong SYC, Davis JS, Eichenberger E, Holland TL, Fowler VG. 2015.
549 *Staphylococcus aureus* Infections: Epidemiology, Pathophysiology, Clinical
550 Manifestations, and Management. *Clin Microbiol Rev* 28:603–661.
- 551 11. Bhattacharya M, Wozniak DJ, Stoodley P, Hall-Stoodley L. 2015. Prevention and
552 treatment of *Staphylococcus aureus* biofilms. *Expert Rev Anti Infect Ther* 13:1499–
553 1516.
- 554 12. Flemming H-C, Wingender J. 2010. The biofilm matrix. *Nat Rev Microbiol* 19:139–
555 150.
- 556 13. O'Neill E, Pozzi C, Houston P, Smyth D, Humphreys H, Robinson DA, O'Gara JP.
557 2007. Association between Methicillin Susceptibility and Biofilm Regulation in
558 *Staphylococcus aureus* Isolates from Device-Related Infections. *J Clin Microbiol*
559 45:1379–1388.
- 560 14. Whitchurch CB. 2002. Extracellular DNA Required for Bacterial Biofilm Formation.
561 *Science* (80-) 295:1487–1487.
- 562 15. Mann EE, Rice KC, Boles BR, Endres JL, Ranjit D, Chandramohan L, Tsang LH,
563 Smeltzer MS, Horswill AR, Bayles KW. 2009. Modulation of eDNA Release and
564 Degradation Affects *Staphylococcus aureus* Biofilm Maturation. *PLoS One*
565 4:e5822.
- 566 16. Das T, Sehar S, Manefield M. 2013. The roles of extracellular DNA in the structural

- 567 integrity of extracellular polymeric substance and bacterial biofilm development.
568 Environ Microbiol Rep 5:778–786.
- 569 17. Cramton SE, Ulrich M, Gotz F, Doring G. 2001. Anaerobic Conditions Induce
570 Expression of Polysaccharide Intercellular Adhesin in *Staphylococcus aureus* and
571 *Staphylococcus epidermidis*. Infect Immun 69:4079–4085.
- 572 18. Vergara-Irigaray M, Maira-Litran T, Merino N, Pier GB, Penades JR, Lasa I. 2008.
573 Wall teichoic acids are dispensable for anchoring the PNAG exopolysaccharide to
574 the *Staphylococcus aureus* cell surface. Microbiology 154:865–877.
- 575 19. Arciola CR, Campoccia D, Ravaioli S, Montanaro L. 2015. Polysaccharide
576 intercellular adhesin in biofilm: structural and regulatory aspects. Front Cell Infect
577 Microbiol 5:1–10.
- 578 20. O’Gara JP. 2007. ica and beyond: biofilm mechanisms and regulation in
579 *Staphylococcus epidermidis* and *Staphylococcus aureus*. FEMS Microbiol Lett
580 270:179–188.
- 581 21. Hussain M, von Eiff C, Sinha B, Joost I, Herrmann M, Peters G, Becker K. 2008.
582 eap Gene as Novel Target for Specific Identification of *Staphylococcus aureus*. J
583 Clin Microbiol 46:470–476.
- 584 22. Haggar A, Hussain M, Lonnie H, Herrmann M, Norrby-Teglund A, Flock J-I. 2003.
585 Extracellular Adherence Protein from *Staphylococcus aureus* Enhances
586 Internalization into Eukaryotic Cells. Infect Immun 71:2310–2317.
- 587 23. Chavakis T, Wiechmann K, Preissner KT, Herrmann M. 2005. *Staphylococcus*

- 588 *aureus* interactions with the endothelium. The role of bacterial “Secretable
589 Expanded Repertoire Adhesive Molecules” (SERAM) in disturbing host defense
590 systems. *Thromb Haemost* 95:715–9.
- 591 24. Johnson M, Cockayne A, Morrissey JA. 2008. Iron-Regulated Biofilm Formation in
592 *Staphylococcus aureus* Newman Requires *ica* and the Secreted Protein Emp.
593 *Infect Immun* 76:1756–1765.
- 594 25. Thompson KM, Abraham N, Jefferson KK. 2010. *Staphylococcus aureus*
595 extracellular adherence protein contributes to biofilm formation in the presence of
596 serum. *FEMS Microbiol Lett* 305:143–147.
- 597 26. Foster TJ, Geoghegan JA, Ganesh VK, Höök M. 2013. Adhesion, invasion and
598 evasion: the many functions of the surface proteins of *Staphylococcus aureus*. *Nat*
599 *Rev Microbiol* 12:49–62.
- 600 27. Mazmanian SK, Ton-That H, Schneewind O. 2001. Sortase-catalysed anchoring of
601 surface proteins to the cell wall of *Staphylococcus aureus*. *Mol Microbiol* 40:1049–
602 1057.
- 603 28. Roche FM. 2003. Characterization of novel LPXTG-containing proteins of
604 *Staphylococcus aureus* identified from genome sequences. *Microbiology* 149:643–
605 654.
- 606 29. Corrigan RM, Rigby D, Handley P, Foster TJ. 2007. The role of *Staphylococcus*
607 *aureus* surface protein SasG in adherence and biofilm formation. *Microbiology*
608 153:2435–2446.

- 609 30. Kuroda M, Ito R, Tanaka Y, Yao M, Matoba K, Saito S, Tanaka I, Ohta T. 2008.
610 *Staphylococcus aureus* surface protein SasG contributes to intercellular
611 autoaggregation of *Staphylococcus aureus*. *Biochem Biophys Res Commun*
612 377:1102–1106.
- 613 31. Geoghegan JA, Corrigan RM, Gruszka DT, Speziale P, O’Gara JP, Potts JR,
614 Foster TJ. 2010. Role of Surface Protein SasG in Biofilm Formation by
615 *Staphylococcus aureus*. *J Bacteriol* 192:5663–5673.
- 616 32. Conrady DG, Brescia CC, Horii K, Weiss AA, Hassett DJ, Herr AB. 2008. A
617 zinc-dependent adhesion module is responsible for intercellular adhesion in
618 staphylococcal biofilms. *Proc Natl Acad Sci* 105:19456–19461.
- 619 33. Formosa-Dague C, Speziale P, Foster TJ, Geoghegan JA, Dufrêne YF. 2016.
620 Zinc-dependent mechanical properties of *Staphylococcus aureus* biofilm-forming
621 surface protein SasG. *Proc Natl Acad Sci* 113:410–415.
- 622 34. Sugimoto S, Sato F, Miyakawa R, Chiba A, Onodera S, Hori S, Mizunoe Y. 2018.
623 Broad impact of extracellular DNA on biofilm formation by clinically isolated
624 Methicillin-resistant and -sensitive strains of *Staphylococcus aureus*. *Sci Rep* 8:1–
625 11.
- 626 35. Sugimoto S, Iwamoto T, Takada K, Okuda K, Tajima A, Iwase T, Mizunoe Y. 2013.
627 *Staphylococcus epidermidis* Esp Degrades Specific Proteins Associated with
628 *Staphylococcus aureus* Biofilm Formation and Host-Pathogen Interaction. *J*
629 *Bacteriol* 195:1645–1655.

- 630 36. Horton RM, Hunt HD, Ho SN, Pullen JK, Pease LR. 1989. Engineering hybrid
631 genes without the use of restriction enzymes: gene splicing by overlap extension.
632 *Gene* 77:61–68.
- 633 37. Bae T, Schneewind O. 2006. Allelic replacement in *Staphylococcus aureus* with
634 inducible counter-selection. *Plasmid* 55:58–63.
- 635 38. Lévesque CM, Voronejskaia E, Huang YC, Mair RW, Ellen RP, Cvitkovitch DG.
636 2005. Involvement of sortase anchoring of cell wall proteins in biofilm formation by
637 *Streptococcus mutans*. *Infect Immun* 73:3773–7.
- 638 39. Franciosa G, Maugliani A, Scalfaro C, Floridi F, Aureli P. 2009. Expression of
639 internalin A and biofilm formation among *Listeria monocytogenes* clinical isolates.
640 *Int J Immunopathol Pharmacol* 22:183–93.
- 641 40. Reardon-Robinson ME, Wu C, Mishra A, Chang C, Bier N, Das A, Ton-That H.
642 2014. Pilus hijacking by a bacterial coaggregation factor critical for oral biofilm
643 development. *Proc Natl Acad Sci* 111:3835–3840.
- 644 41. Sanchez CJ, Shivshankar P, Stol K, Trakhtenbroit S, Sullam PM, Sauer K,
645 Hermans PWM, Orihuela CJ. 2010. The pneumococcal serine-rich repeat protein is
646 an intraspecies bacterial adhesin that promotes bacterial aggregation in Vivo and
647 in biofilms. *PLoS Pathog* 6:33–34.
- 648 42. Rohde H, Burdelski C, Bartscht K, Hussain M, Buck F, Horstkotte MA, Knobloch
649 JKM, Heilmann C, Herrmann M, Mack D. 2005. Induction of *Staphylococcus*
650 *epidermidis* biofilm formation via proteolytic processing of the

- 651 accumulation-associated protein by staphylococcal and host proteases. Mol
652 Microbiol 55:1883–1895.
- 653 43. Kreiswirth BN, Löfdahl S, Betley MJ, O'Reilly M, Schlievert PM, Bergdoll MS,
654 Novick RP. 1983. The toxic shock syndrome exotoxin structural gene is not
655 detectably transmitted by a prophage. Nature 305:709–12.
- 656 44. Eisenbeis J, Saffarzadeh M, Peisker H, Jung P, Thewes N, Preissner KT,
657 Herrmann M, Molle V, Geisbrecht B V., Jacobs K, Bischoff M. 2018. The
658 *Staphylococcus aureus* Extracellular Adherence Protein Eap Is a DNA Binding
659 Protein Capable of Blocking Neutrophil Extracellular Trap Formation. Front Cell
660 Infect Microbiol 8:1–12.
- 661 45. Sugimoto S, Okuda K, Miyakawa R, Sato M, Arita-Morioka K, Chiba A, Yamanaka
662 K, Ogura T, Mizunoe Y, Sato C. 2016. Imaging of bacterial multicellular behaviour
663 in biofilms in liquid by atmospheric scanning electron microscopy. Sci Rep
664 6:25889.
- 665 46. Kaito C, Akimitsu N, Watanabe H, Sekimizu K. 2002. Silkworm larvae as an animal
666 model of bacterial infection pathogenic to humans. Microb Pathog 32:183–190.
- 667 47. Geisbrecht B V., Hamaoka BY, Perman B, Zemla A, Leahy DJ. 2005. The Crystal
668 Structures of EAP Domains from *Staphylococcus aureus* Reveal an Unexpected
669 Homology to Bacterial Superantigens. J Biol Chem 280:17243–17250.
- 670 48. Decker R, Burdelski C, Zobiak M, Büttner H, Franke G, Christner M, Saß K, Zobiak
671 B, Henke HA, Horswill AR, Bischoff M, Bur S, Hartmann T, Schaeffer CR, Fey PD,

- 672 Rohde H. 2015. An 18 kDa Scaffold Protein Is Critical for *Staphylococcus*
673 *epidermidis* Biofilm Formation. PLOS Pathog 11:e1004735.
- 674 49. Merino N, Toledo-Arana A, Vergara-Irigaray M, Valle J, Solano C, Calvo E, Lopez
675 JA, Foster TJ, Penadés JR, Lasa I. 2009. Protein A-mediated multicellular behavior
676 in *Staphylococcus aureus*. J Bacteriol 191:832–843.
- 677 50. Miyazaki S, Matsumoto Y, Sekimizu K, Kaito C. 2012. Evaluation of
678 *Staphylococcus aureus* virulence factors using a silkworm model. FEMS Microbiol
679 Lett 326:116–124.
- 680 51. Pohl K, Francois P, Stenz L, Schlink F, Geiger T, Herbert S, Goerke C, Schrenzel J,
681 Wolz C. 2009. CodY in *Staphylococcus aureus*: a Regulatory Link between
682 Metabolism and Virulence Gene Expression. J Bacteriol 191:2953–2963.
- 683 52. Saravia-Otten P, Müller HP, Arvidson S. 1997. Transcription of *Staphylococcus*
684 *aureus* fibronectin binding protein genes is negatively regulated by *agr* and an
685 *agr*-independent mechanism. J Bacteriol 179:5259–5263.
- 686 53. Xiong Y-Q, Bayer AS, Yeaman MR, Van Wamel W, Manna AC, Cheung AL. 2004.
687 Impacts of *sarA* and *agr* in *Staphylococcus aureus* strain Newman on
688 fibronectin-binding protein A gene expression and fibronectin adherence capacity
689 in vitro and in experimental infective endocarditis. Infect Immun 72:1832–6.
- 690 54. Wolz C, McDevitt D, Foster TJ, Cheung AL. 1996. Influence of *agr* on fibrinogen
691 binding in *Staphylococcus aureus* Newman. Infect Immun 64:3142–7.
- 692 55. Rom JS, Atwood DN, Beenken KE, Meeker DG, Loughran AJ, Spencer HJ, Lantz

- 693 TL, Smeltzer MS. 2017. Impact of *Staphylococcus aureus* regulatory mutations that
694 modulate biofilm formation in the USA300 strain LAC on virulence in a murine
695 bacteremia model. *Virulence* 8:1776–1790.
- 696 56. Ferreira FA, Souza RR, de Sousa Moraes B, de Amorim Ferreira AM, Américo MA,
697 Fracalanza SEL, dos Santos Silva Couceiro JN, Sá Figueiredo AM. 2013. Impact
698 of *agr* dysfunction on virulence profiles and infections associated with a novel
699 methicillin-resistant *Staphylococcus aureus* (MRSA) variant of the lineage
700 ST1-SCC*mec* IV. *BMC Microbiol* 13:93.
- 701 57. Houston P, Rowe SE, Pozzi C, Waters EM, O’Gara JP. 2011. Essential Role for
702 the Major Autolysin in the Fibronectin-Binding Protein-Mediated *Staphylococcus*
703 *aureus* Biofilm Phenotype. *Infect Immun* 79:1153–1165.
- 704 58. Mainiero M, Goerke C, Geiger T, Gonser C, Herbert S, Wolz C. 2010. Differential
705 Target Gene Activation by the *Staphylococcus aureus* Two-Component System
706 *saeRS*. *J Bacteriol* 192:613–623.
- 707 59. Harraghy N, Kormanec J, Wolz C, Homerova D, Goerke C, Ohlsen K, Qazi S, Hill P,
708 Herrmann M. 2005. *sae* is essential for expression of the staphylococcal adhesins
709 Eap and Emp. *Microbiology* 151:1789–800.
- 710 60. Chiba A, Sugimoto S, Sato F, Hori S, Mizunoe Y. 2015. A refined technique for
711 extraction of extracellular matrices from bacterial biofilms and its applicability.
712 *Microb Biotechnol* 8:392–403.
- 713 61. Cui L, Neoh H, Iwamoto A, Hiramatsu K. 2012. Coordinated phenotype switching

- 714 with large-scale chromosome flip-flop inversion observed in bacteria. Proc Natl
715 Acad Sci 109:E1647–E1656.
- 716 62. Schenk S, Laddaga RA. 1992. Improved methodd for electroporation of
717 *Staphylococcus aureus*. FEMS Microbiol Lett 94:133–138.
- 718 63. Kaplan JB, Rangunath C, Ramasubbu N, Fine DH. 2003. Detachment of
719 *Actinobacillus actinomycetemcomitans* Biofilm Cells by an Endogenous
720 β -Hexosaminidase Activity. J Bacteriol 185:4693–4698.
- 721 64. Sugimoto S, Arita-Morioka K, Mizunoe Y, Yamanaka K, Ogura T. 2015. Thioflavin
722 T as a fluorescence probe for monitoring RNA metabolism at molecular and cellular
723 levels. Nucleic Acids Res 43:e92–e92.
- 724 65. Kanda Y. 2013. Investigation of the freely available easy-to-use software 'EZR' for
725 medical statistics. Bone Marrow Transplant 48:452–458.
- 726

727 **Figure legends**

728 **FIG 1** Eap and SrtA play redundant roles in biofilm formation. (A) Biomasses of biofilms
729 formed by MR23 wild-type (WT), Δeap , $\Delta srtA$, and $\Delta eap \Delta srtA$ strains grown in BHIG at
730 37°C for 24 h were determined by crystal violet staining. (B) Reduced biomass of Δeap
731 $\Delta srtA$ strain biofilm was complemented by providing plasmid-encoded Eap or SrtA.
732 Empty vector (pLC1) was introduced into WT and $\Delta eap \Delta srtA$ strains as a positive and
733 negative control, respectively. The data are presented relative to the positive control,
734 designated as 100%. (A, B) The means and standard deviations of biofilm biomass from
735 three independent experiments are shown. **, $P < 0.01$; NS, not significant. (C) Protein
736 profiles of ECM isolated from WT pLC1, $\Delta eap \Delta srtA$ pLC1, $\Delta eap \Delta srtA$ pEap, and Δeap
737 $\Delta srtA$ pSrtA strains were analyzed by SDS-PAGE with Coomassie Brilliant Blue (CBB)
738 staining. Prominent bands indicated by an arrowhead correspond to Eap (35). (D) Cell
739 wall fractions of the indicated strains were analyzed by SDS-PAGE with CBB staining.
740 The images are representative of at least three independent analyses.

741

742 **FIG 2** Identification of CWAPs responsible for biofilm formation in MR23. (A, B)

743 Biomasses of biofilms produced by the indicated strains were quantified as described in

744 Fig. 1. The means and standard deviations of biofilm biomasses from three independent

745 experiments are shown. **, $P < 0.01$; NS, not significant. (C) Protein profiles of ECM
746 isolated from the indicated strains were analyzed by SDS-PAGE with CBB staining. (D)
747 Proteins in the cell wall fractions of the indicated strains were subjected to SDS-PAGE
748 with CBB staining, or western blotting with anti-SasG antibody.

749

750 **FIG 3** SasG is a DNA-binding protein. (A) DNase I-sensitivities of the biofilms formed by
751 the indicated strains are shown. Relative biofilm biomasses are shown (non-treated
752 biofilms are defined as 100%). Original data are shown in Figure S1. -, absence; +,
753 presence. (B) DNA-binding capacity of SasG was analyzed by gel shift assay. Purified
754 SasG (0.1, 0.5, and 1 μM) was mixed with lambda DNA (λDNA) prior to agarose gel
755 electrophoresis. (C) Degradation of λDNA by DNase I was analyzed in the presence and
756 absence of purified SasG. After the treatment, DNase I and SasG were degraded by
757 proteinase K, and the residual DNA was analyzed by agarose gel electrophoresis. Band
758 intensities were measured using LAS-4000 Image Analyzer and the relative intensities
759 are shown in the graph.

760

761 **FIG 4** LPXTG motif in SasG plays a role in compensating for the loss of Eap in biofilm
762 formation. (A) The domain structure of MR23 SasG. S, signal peptide; A, A domain; B, B

763 domain; and LPXTG, LPXTG motif. Plasmids for the expression of SasG^{WT} and SasG^{ΔL}
764 were constructed in the current study (Table S1). (B) Biomass of biofilms produced by the
765 indicated strains was determined as described in Fig. 1. The means and standard
766 deviations from three independent experiments are shown. **, $P < 0.01$. (C, D) SasG
767 proteins in the cell wall fractions (C) and culture supernatants (D) were analyzed by
768 western blotting using anti-SasG antibody.

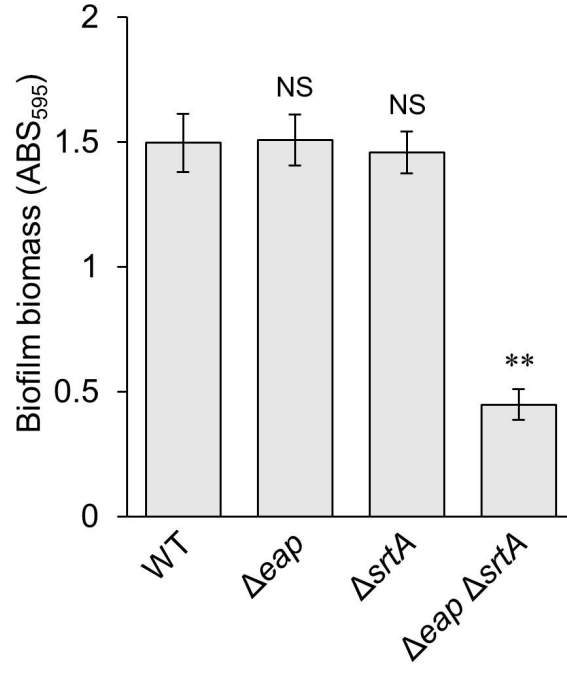
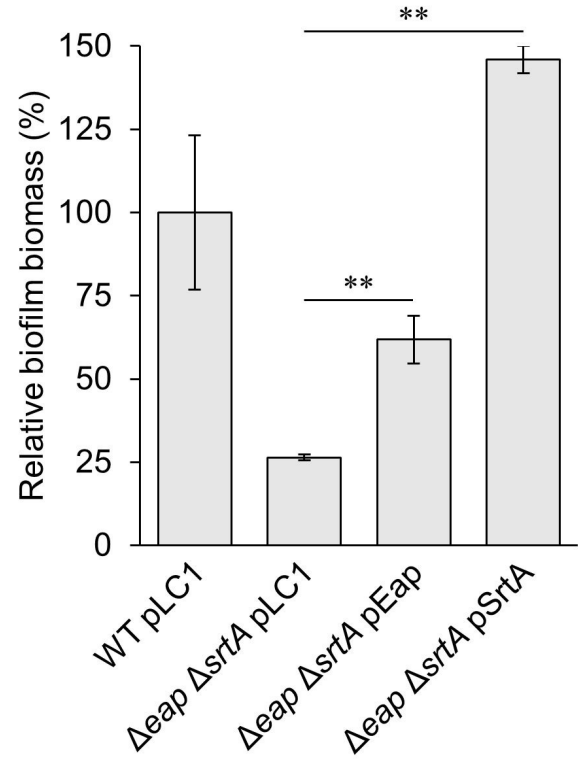
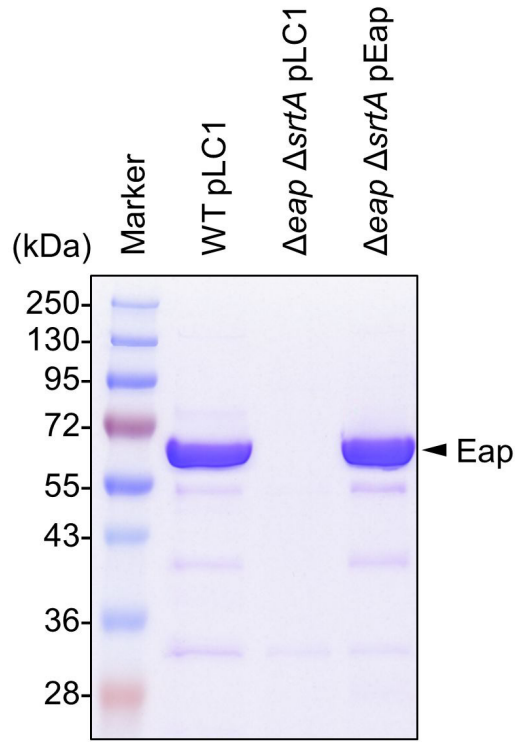
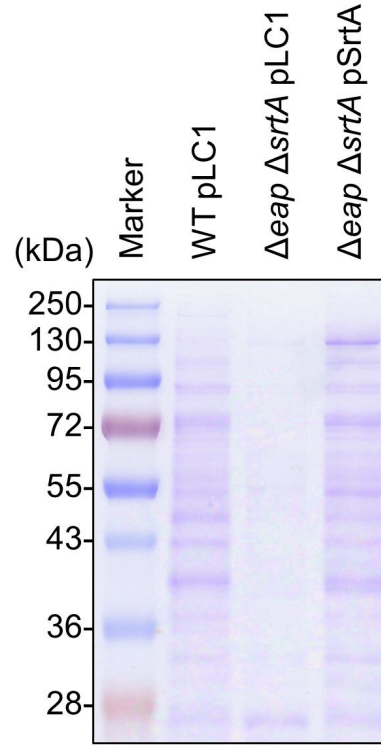
769

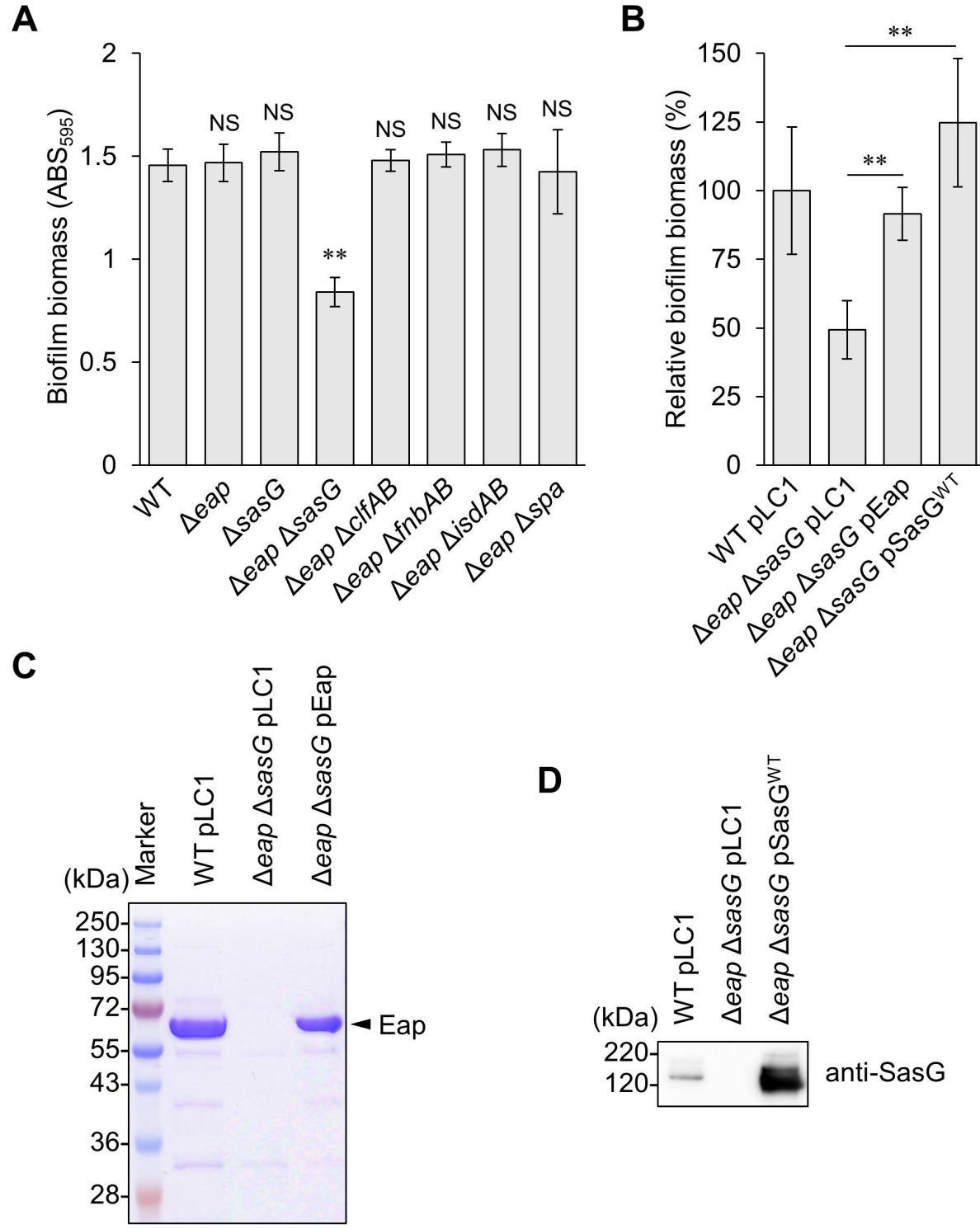
770 **FIG 5** Three-dimensional structure of bacterial biofilms. (A) Biofilms formed by the
771 indicated strains were stained with thioflavin T and analyzed using CLSM. Typical top
772 oblique and side views of the biofilms are shown. (B) Thickness of the biofilms formed in
773 three independent dishes was determined using Image J software. The line in each box
774 and whisker plot represents the median thickness of biofilms formed by the indicated
775 strains. O, outlying values; **, $P < 0.01$; NS, not significant.

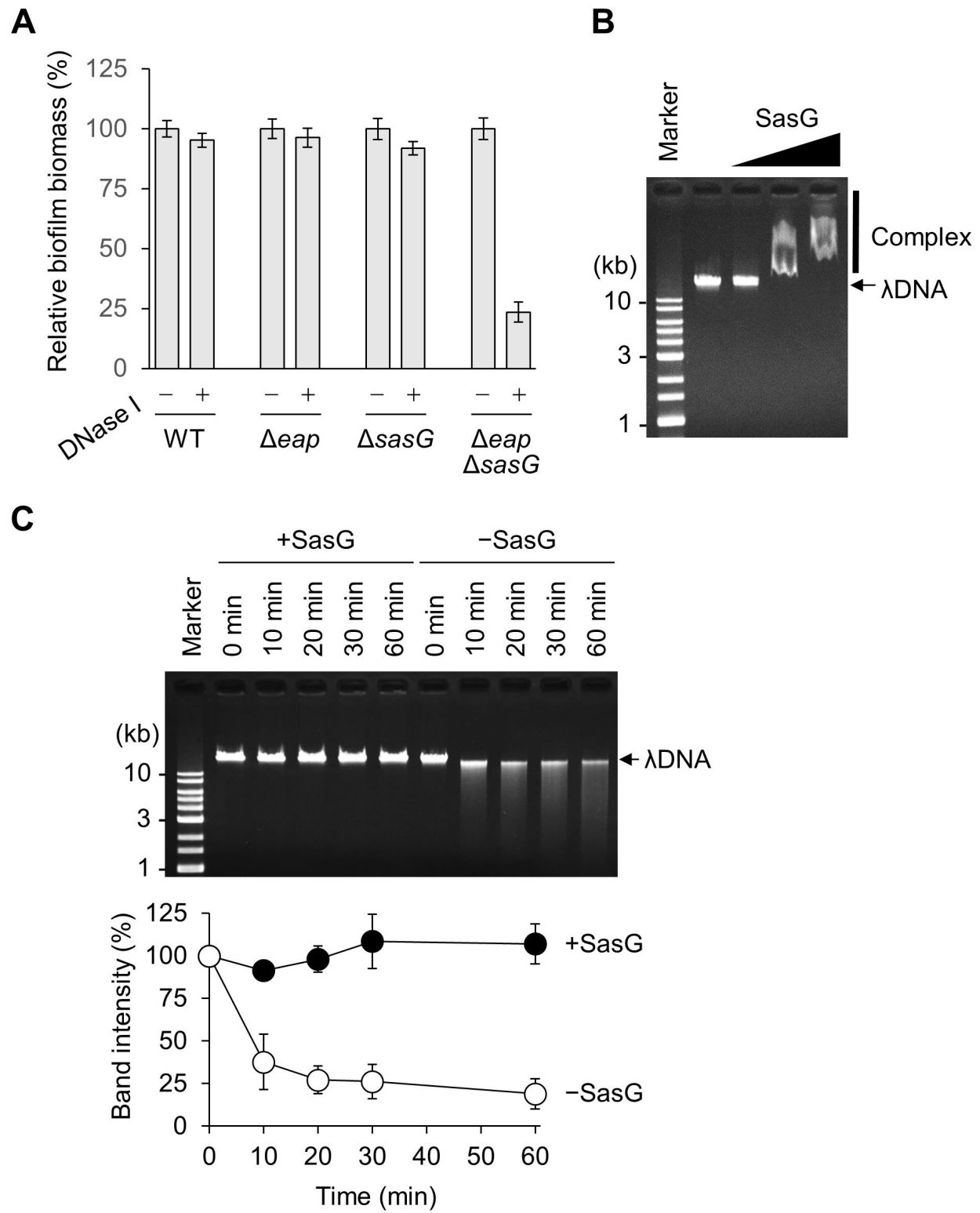
776

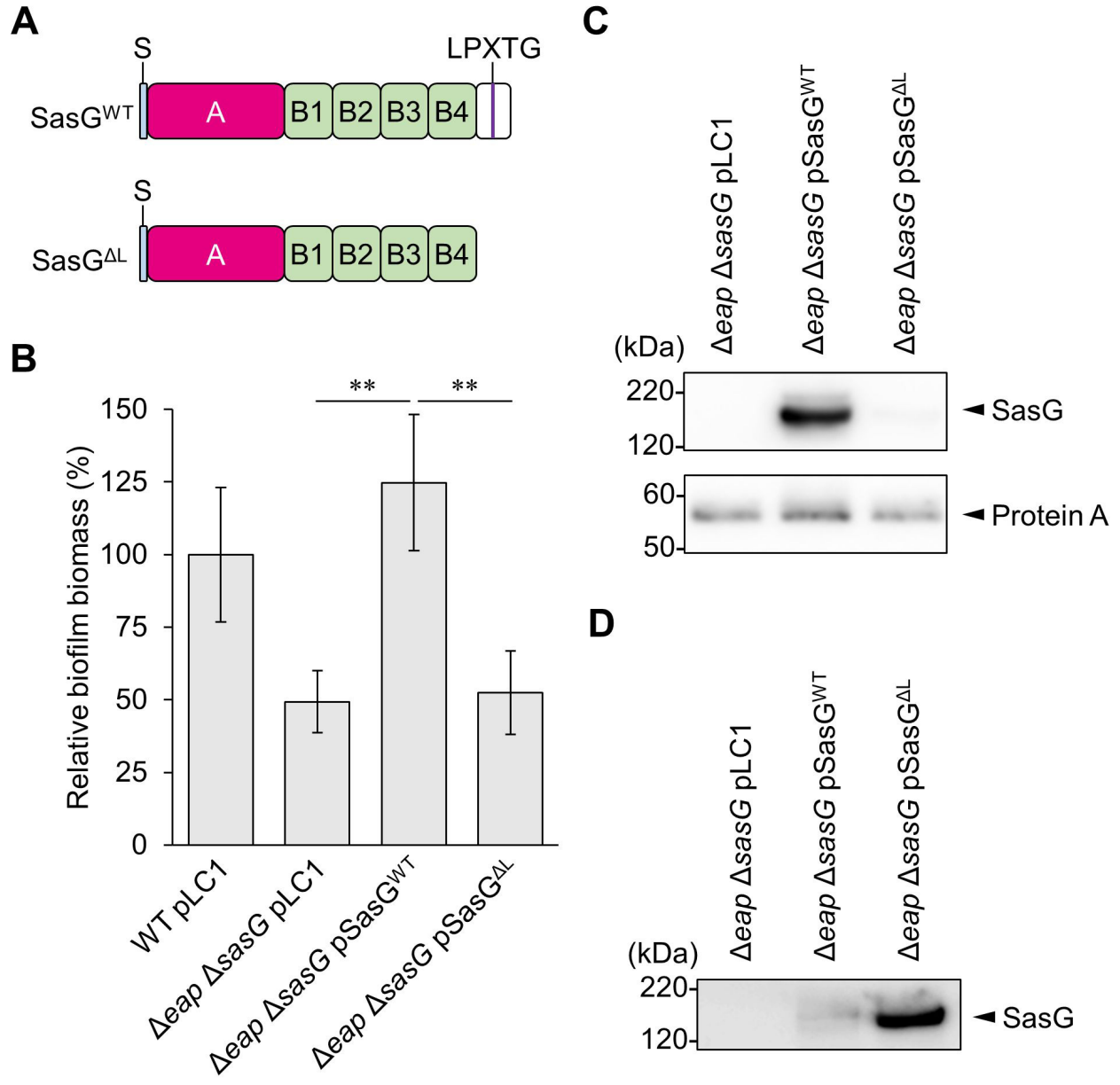
777 **FIG 6** Evaluation of the pathogenicity of *S. aureus* strains in silkworm larvae. Ten
778 silkworm larvae were injected with diluted overnight cultures (1×10^7 CFU) of the
779 indicated strains. Larval survival was monitored at 25°C for 60 h. The curves are
780 representative of at least three independent experiments. The differences between WT

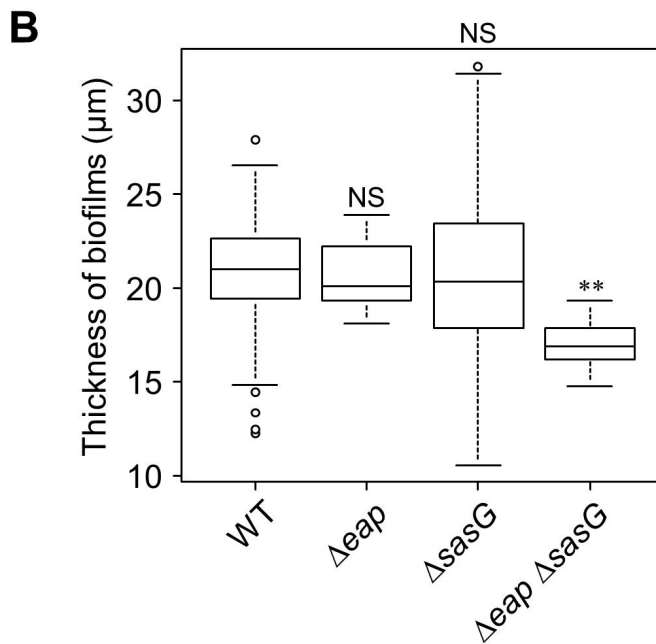
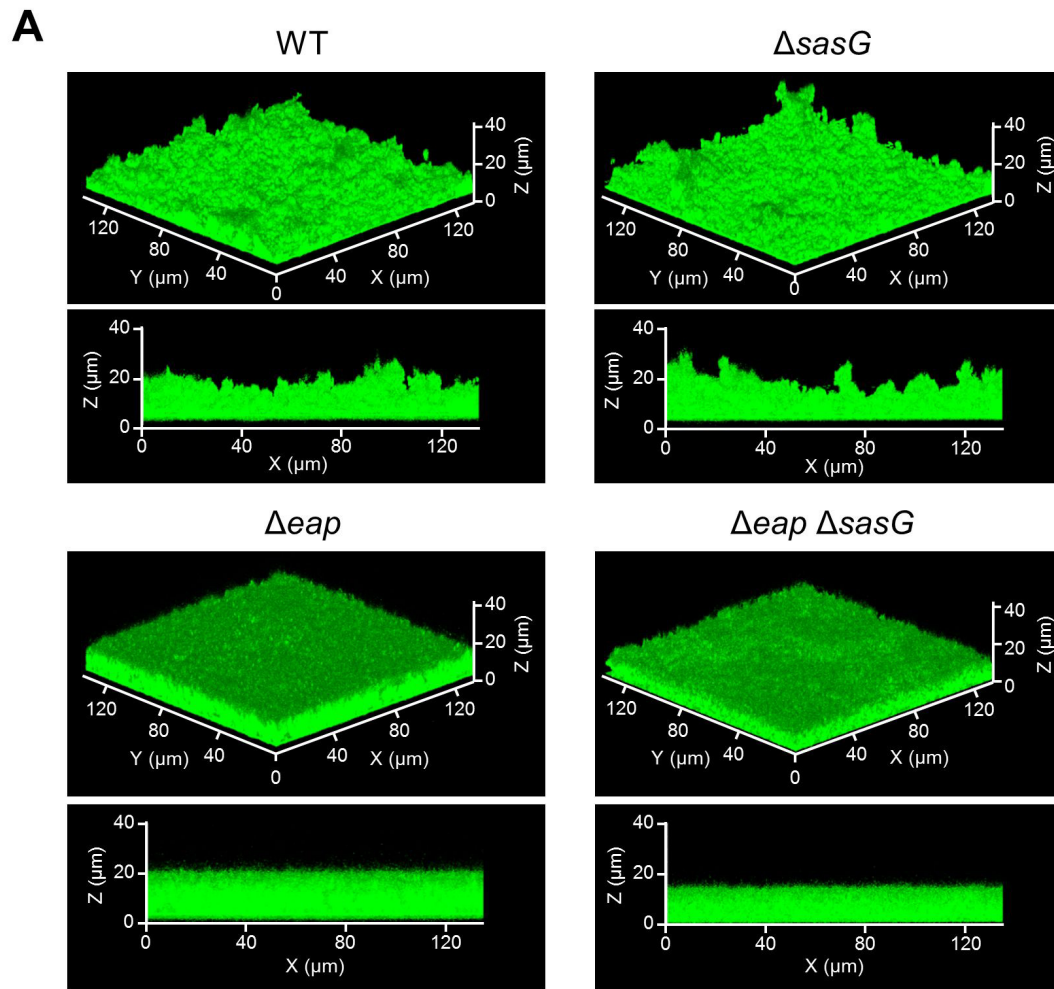
781 and Δeap $\Delta sasG$ strains, or between WT and the injection control (0.6% NaCl solution)
782 were statistically significant ($P < 0.05$ and $P < 0.01$, respectively). By contrast, no
783 statistical difference was apparent between WT and Δeap strain treatments, or between
784 WT and $\Delta sasG$ strain treatments ($P > 0.05$).

Yonemoto *et al.* Figure 1**A****B****C****D**

Yonemoto *et al.* Figure 2

Yonemoto *et al.* Figure 3

Yonemoto *et al.* Figure 4

Yonemoto *et al.* Figure 5

Yonemoto *et al.* Figure 6